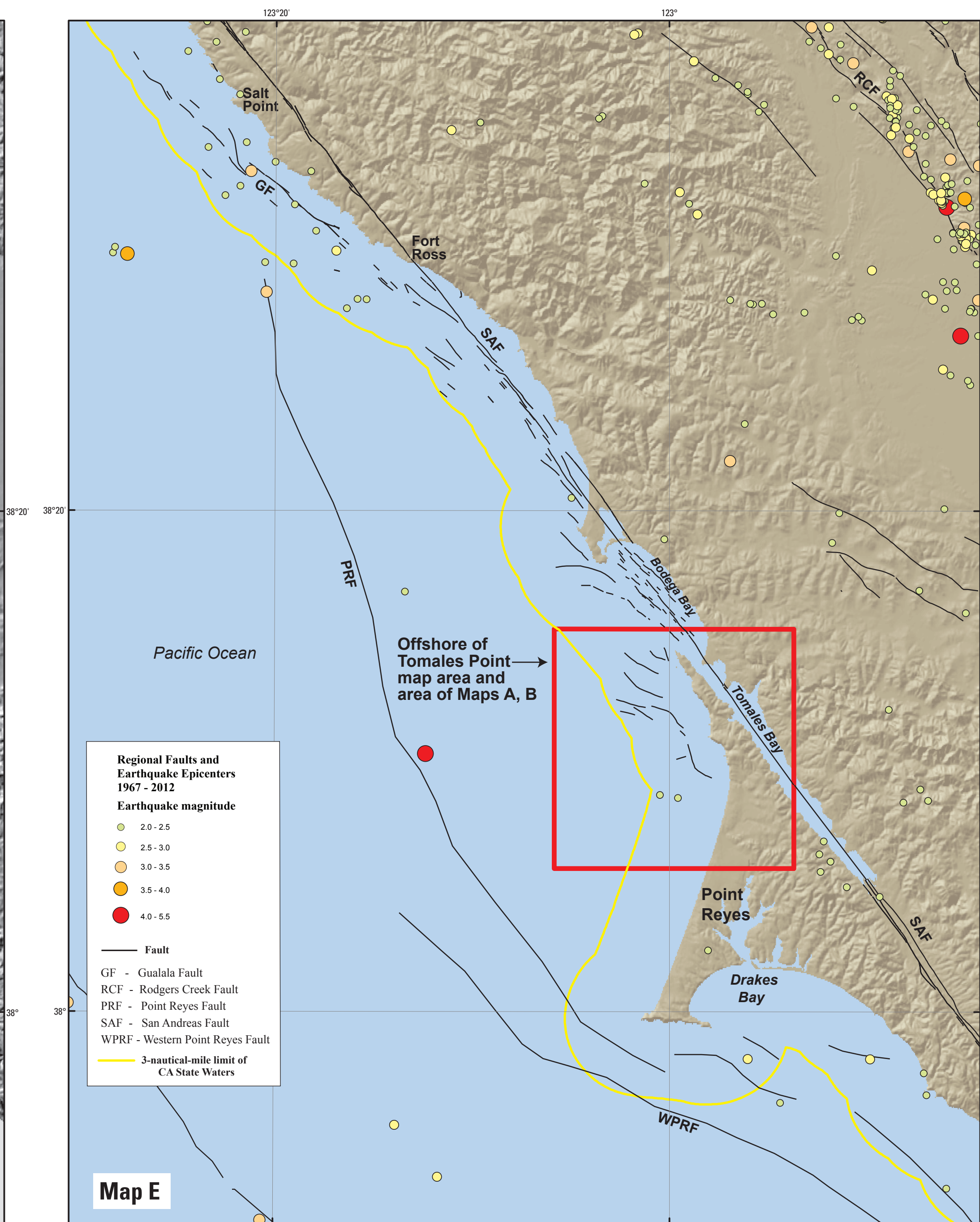
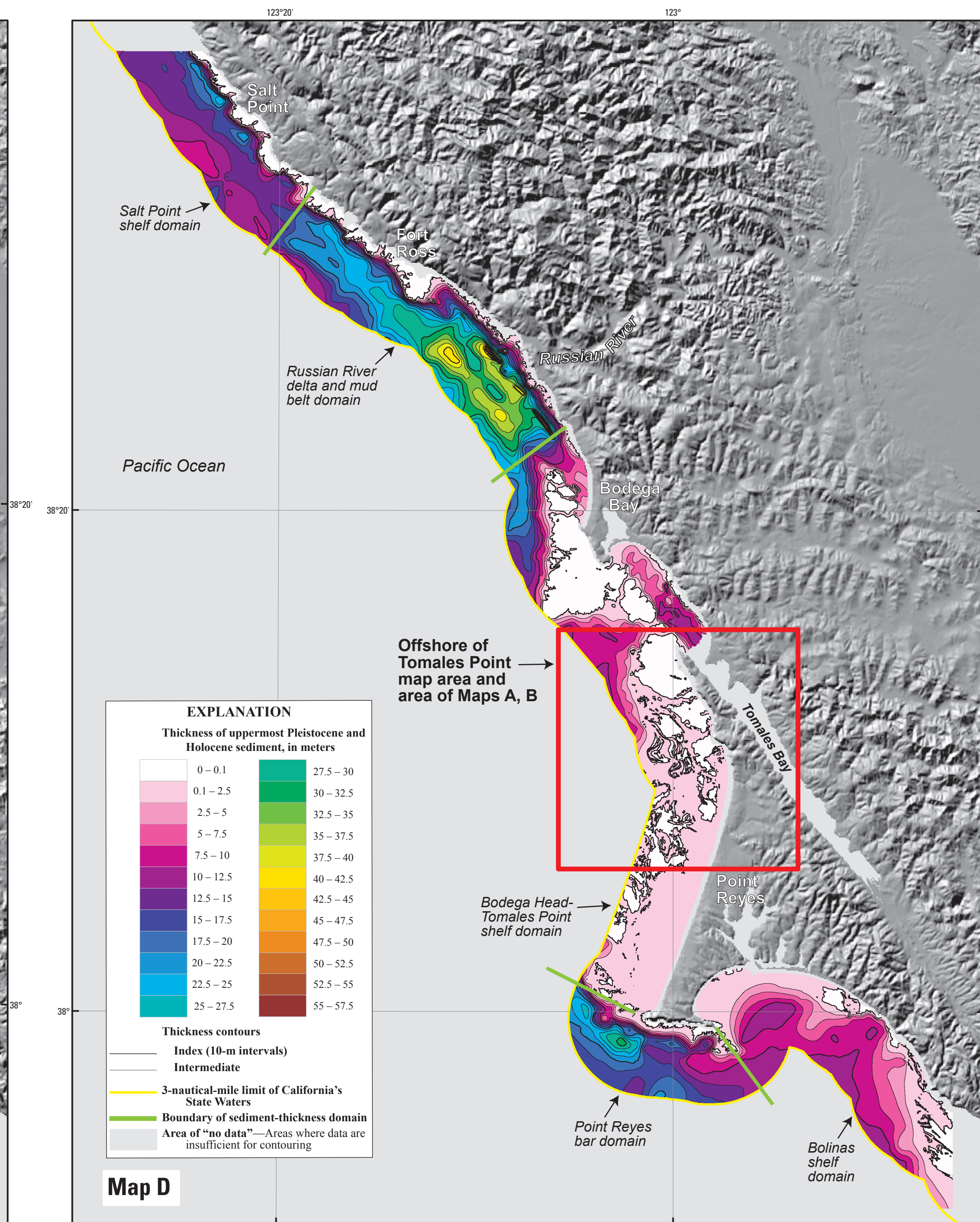
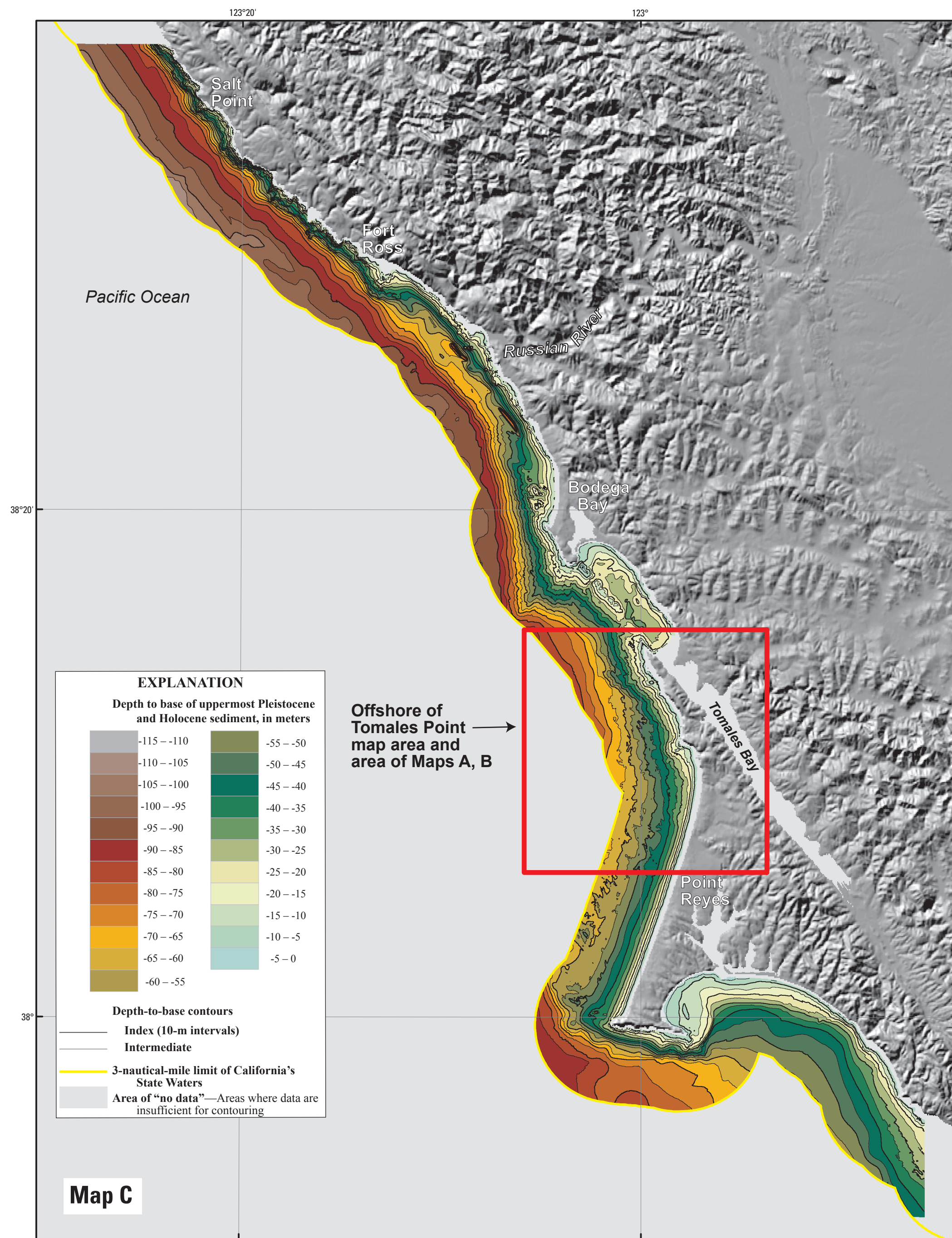


Derives elevation data from California Coastal Commission, available at <http://www.ccc.ca.gov/geographic-information/coordinates/>, and from U.S. Geological Survey, National Elevation Dataset, available at <http://ned.srs.gov/>. California's State Waters limit from NOAA Office of Coast Survey  
Vertical datum: National Mean Sea Level  
NOT INTENDED FOR NAVIGATIONAL USE

Depth and thickness mapped by Samuel Y. Johnson and Stephen R. Hartwell, 2015-2015  
GIS database and digital cartography by Stephen R. Hartwell

Depth and thickness mapped by Samuel Y. Johnson and Stephen R. Hartwell, 2015-2015  
GIS database and digital cartography by Stephen R. Hartwell



Derives topography from the U.S. Geological Survey, 2012 National Elevation Dataset  
Universal Transverse Mercator projection, Zone 10N  
NOT INTENDED FOR NAVIGATIONAL USE

Depth and thickness mapped by Samuel Y. Johnson and Stephen R. Hartwell, 2015-2015  
GIS database and digital cartography by Stephen R. Hartwell  
Manuscript approved for publication May 4, 2015

Depth and thickness mapped by Samuel Y. Johnson and Stephen R. Hartwell, 2015-2015  
GIS database and digital cartography by Stephen R. Hartwell  
Manuscript approved for publication May 4, 2015

This sheet includes maps that show the thickness and the depth to base of uppermost Pleistocene and Holocene deposits for the Offshore of Tomales Point area (Maps A, B), as well as for a larger area that extends about 115 km along the coast from Salt Point to Drakes Bay (Maps C, D) to establish a regional context. The uppermost stratigraphic unit (blue shading on the seismic-reflection profiles on sheet 8 of this report) is inferred to have been deposited during the post-Last Glacial Maximum (LGM) sea-level rise in the last 21,000 years (see, for example, Fisher and Fairbanks, 2000). The unit is commonly characterized either by "acoustic transparency" or by parallel, low-amplitude, low-to-high-frequency, continuous to moderately continuous reflections (terminology from Michum and others, 1977). The acoustic transparency can be caused by extensive wave winnowing, which results in uniform sediment grain size and consequent lack of acoustic-impedance contrasts needed to produce seismic reflections. On the continental shelf, the contact with underlying units is a transgressive surface of erosion commonly marked by angularity, channeling, or a distinct upward change to lower amplitude, more diffuse reflections.

In the northern part of this region (Offshore of Salt Point map area), the sequence of uppermost Pleistocene and Holocene deposits, which has a prominent unconformity, includes a lower, older stratigraphic unit, made up of a downlapping sediment wedge that formed along the southwest flank of northern bedrock outcrops. Stratigraphic position, depth of occurrence, and reflection geometry suggest that this lower unit formed during the latter stages of the pre-LGM sea-level fall (about 30,000 to 21,000 years ago). Because this unit and overlying post-LGM deposits each comprise unconsolidated sediments and together overlie a prominent unconformity, our regional thickness and depth-to-base maps (Maps C, D) combine these units in this northern part of the Salt Point to Drakes Bay region.

To make these maps, water bottom and depth to base of the uppermost Pleistocene and Holocene horizons were mapped from seismic-reflection profiles (fig. 1; see also, sheet 8). The difference in the two horizons was reported for every shot point as XY coordinates (UTM zone 10) and two-way travel time (TW). The thickness of the uppermost Pleistocene and Holocene unit (Map B, D) was determined by applying a sound velocity of 1,600 m/sec to the TW. The thickness points were interpolated to a preliminary continuous surface, overlaid with zero-thickness bedrock outcrops (see sheet 10), and contoured following the methods outlined in Wong and others (2012).

The thickness data points are dense along tracklines (about 1 m apart) and sparse between tracklines (1 to 3 km apart), resulting in minor contouring artifacts. To incorporate the effect of a few rapid thickness changes along faults, to remove irregularities from interpolation, and to reflect other geologic information and complexity, the resulting interpolated contours were modified. Contour modifications and regriding were repeated several times to produce the final regional sediment-thickness maps (Maps B, D). Information for the depth to base of the uppermost Pleistocene and Holocene unit (Map A, C) was generated by adding the thickness data to water depths determined by multibeam bathymetry (see sheet 1).

The thickness of the uppermost Pleistocene and Holocene sediments in the offshore of Tomales Point map area ranges from 0 to 11 meters (Map B), and the depth to base of the unit ranges from about 10 to 85 meters (Map A). Mean sediment thickness for the map area is 2.3 m and total sediment volume is 253-106 m<sup>3</sup> (table 7-1 in pamphlet). The thickest sediment occurs along the northern map boundary, at the mouth of Tomales Bay and at water depths of about 60 to 75 m due west of Tomales Point. These two areas are connected and represent upper and lower reaches of a now-submerged channel system that provided an outlet for Tomales Bay and small coastal drainages north of the map area during sea-level lowstand (Maps B, D).

To the south, Cretaceous granitic and Tertiary sedimentary rock crop out on the seafloor or are buried by only a thin cover (mostly less than 2.5 m) of uppermost Pleistocene and Holocene sediment. This thin cover results from a combination of factors including active uplift of the Point Reyes Peninsula (Groves and others, 2010), high wave energy, and very limited sediment supply. Tomales Point blocks southward littoral drift, and west-facing coastal watersheds on this part of the Point Reyes Peninsula are very small, therefore, much of the relatively meager sediment that is present on the shelf could be derived from erosion of local coastal bluffs and sand dunes.

Five different "domains" of sediment thickness are recognized on the regional sediment-thickness maps (table 7-1 in pamphlet, Map D), each with distinctive geologic controls: (1) The Salt Point shelf domain, located in the far northwestern part of the region has a mean sediment thickness of 11.7 m. The thickest sediment (20 to 25 m) is found where a pre-LGM, regressive, downlapping sediment wedge formed above a break in slope that is controlled by a contact between harder bedrock and softer, folded, Pleistocene strata. Sediment thinning in this domain in the outer portions of California's State Waters is the result of a relative lack of sediment supply from local watersheds, as well as a more distal Russian River delta and mid-belt domain, located offshore of the largest sediment source on this part of the coast, has the thickest uppermost Pleistocene and Holocene sediment in the region (mean thickness, 2.1 m). The northward extension into the mid-belt "mead belt" results from northward shelf-bottom currents and accretion (Drake and Cacchione, 1985). This domain includes a section of the San Andreas Fault Zone (Map E), which here is characterized by several releasing, right-stepping strands that bound narrow, elongate, pull-apart basins. These sedimentary basins contain the greatest thickness of uppermost Pleistocene and Holocene sediment (about 56 m) in the region. (3) The Bodega Head-Tomales Point shelf domain, located between Bodega Head and the Point Reyes headland, contains the least amount of sediment in the region (mean thickness of 3.4 m). The lack of sediment results from decreased "accommodation space" (note shallower depth contours on Maps A and C) and limited sediment supply. (4) The Point Reyes bar domain, located west and south of the Point Reyes headland, is a local zone of increased sediment thickness (mean thickness of 4.3 m) created by bar deposition on the more protected flank of the Point Reyes headland during rising sea level. (5) The Bolinas shelf domain, located east and southeast of the Point Reyes headland, has a thin sediment cover from limited mean thickness accommodation space caused by tectonic uplift (water depths in this domain within California's State Waters are less than 45 m) as well as limited sediment supply and the high wave energy that is capable of erasing and transporting shelf sediment to deeper water.

Map 5 shows the regional pattern of major faults and earthquakes occurring between 1967 and March 2012 that have inferred or measured magnitudes of 2.0 and greater. Fault locations, which have been simplified, are compiled from interpretation of regional multi-channel industry seismic data, our mapping within California's State Waters (for example, sheet 10), (McCulloch, 1987), and the Quaternary fault and fold database (U.S. Geological Survey, 2010). Earthquake epicenters are from the Northern California Earthquake Data Center (2012), which is maintained by the U.S. Geological Survey and the University of California, Berkeley, Seismological Laboratory, all events of magnitude 2.0 and greater for the time period 1967 through March 2012 are shown. The largest earthquake in the map area (M2.1, 11/16/1978), occurred about 3 km offshore of the Point Reyes Peninsula. There has been a notable lack of microseismicity on this section of the San Andreas Fault since the great 1906 California earthquake (M7.8, 4/18/1906), thought to have nucleated on the San Andreas Fault offshore of San Francisco (fig. 1-1 in pamphlet, Bolt, 1968; Lomas, 2005).

**REFERENCES CITED**

Bolt, B.A., 1968. The focus of the 1906 California earthquake. *Bulletin of the Seismological Society of America*, v. 58, p. 457-471.

Drake, D.E., and Cacchione, D.A., 1985. Seasonal variation in sediment transport on the Russian River shelf, California. *Continental Shelf Research*, v. 4, p. 495-514. doi:10.1016/0278-4343(85)90007-X.

Grove, K., Sklar, L.S., Scherer, A.M., Lee, G., and Davis, J., 2010. Accelerating and spatially-varying crustal uplift and its geomorphic expression, San Andreas Fault zone north of San Francisco, California. *Tectonophysics*, v. 495, p. 236-248. doi:10.1016/j.tecto.2010.09.014.

Lomas, A., 2005. A reanalysis of the hypocentral location and related observations for the Great 1906 California earthquake. *Bulletin of the Seismological Society of America*, v. 95, p. 801-817. doi:10.1785/0120040141.

McCulloch, D.S., 1987. Regional geology and hydrocarbon potential of offshore central California, in Schol, D.W., Grantz, A., and Vedler, J.G., eds., *Geology and Resource Potential of the Continental Margin of Western North America and Adjacent Ocean Basins—Beaufort Sea to Baja California*. Houston, Texas, Circum-Pacific Council for Energy and Mineral Resources, Earth Science Series, v. 4, p. 355-401.

Michum, R.M., Jr., Vail, P.R., and Sangree, J.B., 1977. Seismic stratigraphy and global changes of sea level, part 6—Stratigraphic interpretation of seismic reflection patterns in depositional sequences, in Payton, C.E., ed., *Seismic Stratigraphy—Applications to Hydrocarbon Exploration*. Tulsa, Oklahoma, American Association of Petroleum Geologists, p. 117-133.

Northern California Earthquake Data Center, 2012. Northern California earthquake catalog: Northern California Earthquake Data Center database, accessed April 5, 2012, at <http://www.nceed.ucdavis.edu/>.

Pelner, W.K., and Fairbanks, R.G., 2006. Global glacial ice volume and Last Glacial Maximum duration from an extended Boreas sea level record. *Quaternary Science Reviews*, v. 25, p. 1322-1337. doi:10.1016/j.quascirev.2006.04.010.

U.S. Geological Survey and California Geological Survey, 2010. Quaternary fault and fold database of the United States. U.S. Geological Survey database, accessed April 5, 2012 at <http://earthquake.usgs.gov/hazards/qfaults/>.

Wong, F.L., Phillips, E.L., Johnson, S.Y., and Sliter, R.W., 2012. Modeling of depth to base of Last Glacial Maximum and seafloor sediment thickness for the California State Waters Map Series, eastern Santa Barbara Channel, California. U.S. Geological Survey Open-File Report 2012-1161, 16 p., available at <http://pubs.usgs.gov/ofr/2012/1161/>.